

# The microstructure and the morphology of a Ni-P layer irradiated by a high current pulsed electron beam

Jinglong Gao, Qigang Xun, Yanhui Liu ✉

School of Material Science and Engineering, Shenyang Ligong University, Shenyang, Liaoning 110168, People's Republic of China

✉ E-mail: liouyh@126.com

Published in Micro & Nano Letters; Received on 25th April 2017; Revised on 28th June 2017; Accepted on 10th July 2017

The electroless Ni-P plating on LY12 substrate was irradiated by a low-energy high-current pulsed electron beam (LEHCEB) to form an intermetallic compound. The microstructure and the morphology of the Ni-P layer after surface treatment were investigated. The results show that the Ni-P layer was melted into low viscosity liquid and quickly moved to a wide variety of shapes and sizes under irradiation of the LEHCEB. X-ray diffraction, energy dispersive spectroscopy and scanning electron microscope were employed to detect intermetallic compounds formed from aluminium–nickel systems including  $\text{Al}_3\text{Ni}$ ,  $\text{AlNi}_3$  and  $\text{Al}_3\text{Ni}_2$ .

**1. Introduction:** Intermetallics from aluminium–nickel (Al–Ni) systems have found applications in industrial sources, due to their desirable properties, such as low density, high strength, as well as high corrosion and oxidation resistance [1, 2]. Hence, the formation sequences and growth mechanism of Ni–Al phases have been extensively studied [1]. Several methods have been developed to prepare Al–Ni intermetallics, such as melting, casting, mechanical alloying, powder metallurgy and combustion synthesis. However, by melting and casting methods, which are frequently used for fabrication of Ni–Al, it always brings problems resulting from the large difference between the melting point of Ni and Al and/or possible oxidation and evaporation [3]. The mechanical alloying and powder metallurgy need long processing time. Whilst by combustion synthesis, products are with high porosity [4]. Therefore, it is a challenge to develop a novel approach to fabricate Al–Ni intermetallics on surface, neither using high temperature nor chemical reagents.

In recent years, high-current pulsed electron beam (HCPEB) technique is attracting increasing attention due to its revolutionary functionality such as high efficiency, simplicity and reliability. Especially, during the HCPEB irradiation, the surface of materials would generate a dynamic temperature field within a short-pulse of microsecond level ( $\sim 10^8$  K/s) to melting or evaporation [5]. As an efficient method for surface treatment of materials, HCPEB has been widely used and there have been a number of successful applications of the HCPEB technique to various metals and alloys, which give rise to the formation of non-equilibrium surface microstructure accompanied by modified properties [6–12]. In this Letter, the electroless Ni-P layer was deposited on the LY12 Al substrate and then irradiated by HCPEB. When irradiated by HCPEB, Ni-P layer and the substrate surface were melted and solidified to a compound layer.

Although some efforts have been made to prepare Al–Ni intermetallic compound, the main aim of this study is to afford a lower cost, convenient method and investigate the microstructure of HCPEB surface treated Ni-P layer. In order to obtain a proper perspective on the effect of the HCPEB processing on the microstructure morphology, the change of surface microstructures and the crystalline phase of the specimen, scanning electron microscope (SEM), energy dispersive spectroscopy (EDS) and X-ray diffraction (XRD) were employed.

**2. Experimental:** The substrate material was LY12 Al alloy and the chemical composition (wt%) was as following: Cu=3.8–4.9%,

Mg=1.2–1.8%, Mn=0.0–0.9%, Fe=0.5%, Si=0.5%, Zn=0.25%, Ti=0.15% and Al=balance. The samples were cut to a dimension of 15 mm × 10 mm × 3 mm.

LY12 Al alloy was polished with SiC paper, rinsed and then immersed in an activation bath and then the specimen was electroless plated a nickel phosphorus layer. The constituents of the activation solution, electroless nickel phosphorus plating bath are shown in Table 1. The activated samples were washed with deionised water after each treatment and immersed immediately in the electroless plating bath without drying.

The electron-beam treatment was carried out by electron accelerator SOLO from Russia. Test samples were mounted along the beam's axis so the irradiation was carried out by its

**Table 1** Bath composition and operation conditions for activation and electroless Ni-P bath

Process	Batch composition	Concentration, g L <sup>-1</sup>	Condition
activation	$\text{NH}_4\text{H}_2\text{PO}_4$	85	85°C
	$\text{NH}_4\text{F}$	20	10 min
	$\text{KMnO}_4$	1.4	
	$\text{Na}_3\text{PO}_4$	100	
electroless plating	$\text{NiSO}_4$	25	85°C
	$\text{CH}_3\text{CHOHCOOH}$	25	10 min
	$\text{Na}_2\text{PO}_3$	30	PH 6
	$\text{NH}_4\text{HF}_2$	10	

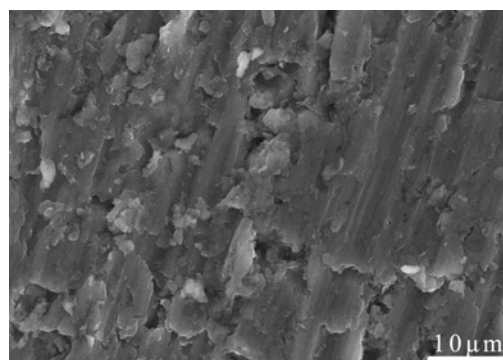


**Fig. 1** Surface morphology image of initial LY12 Al alloy

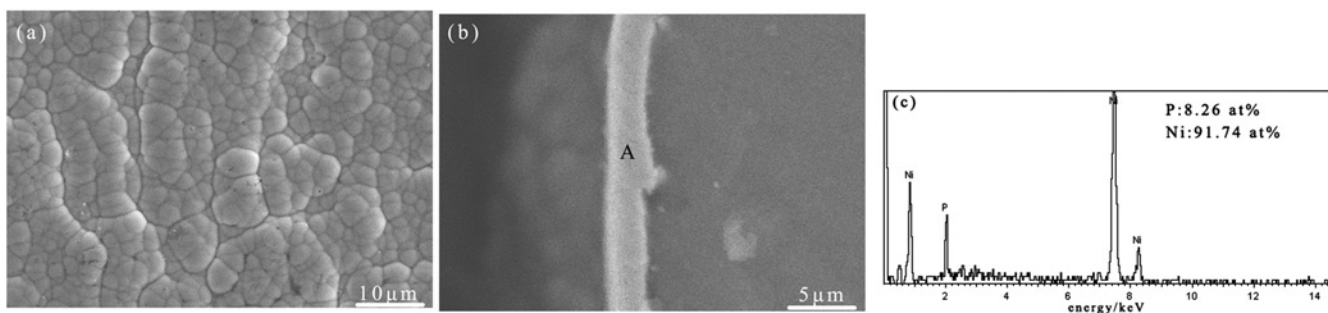


**Fig. 2** SEM images of Ni-P layer  
*a* Surface area  
*b* Cross-section area and  
*c* EDS of point A

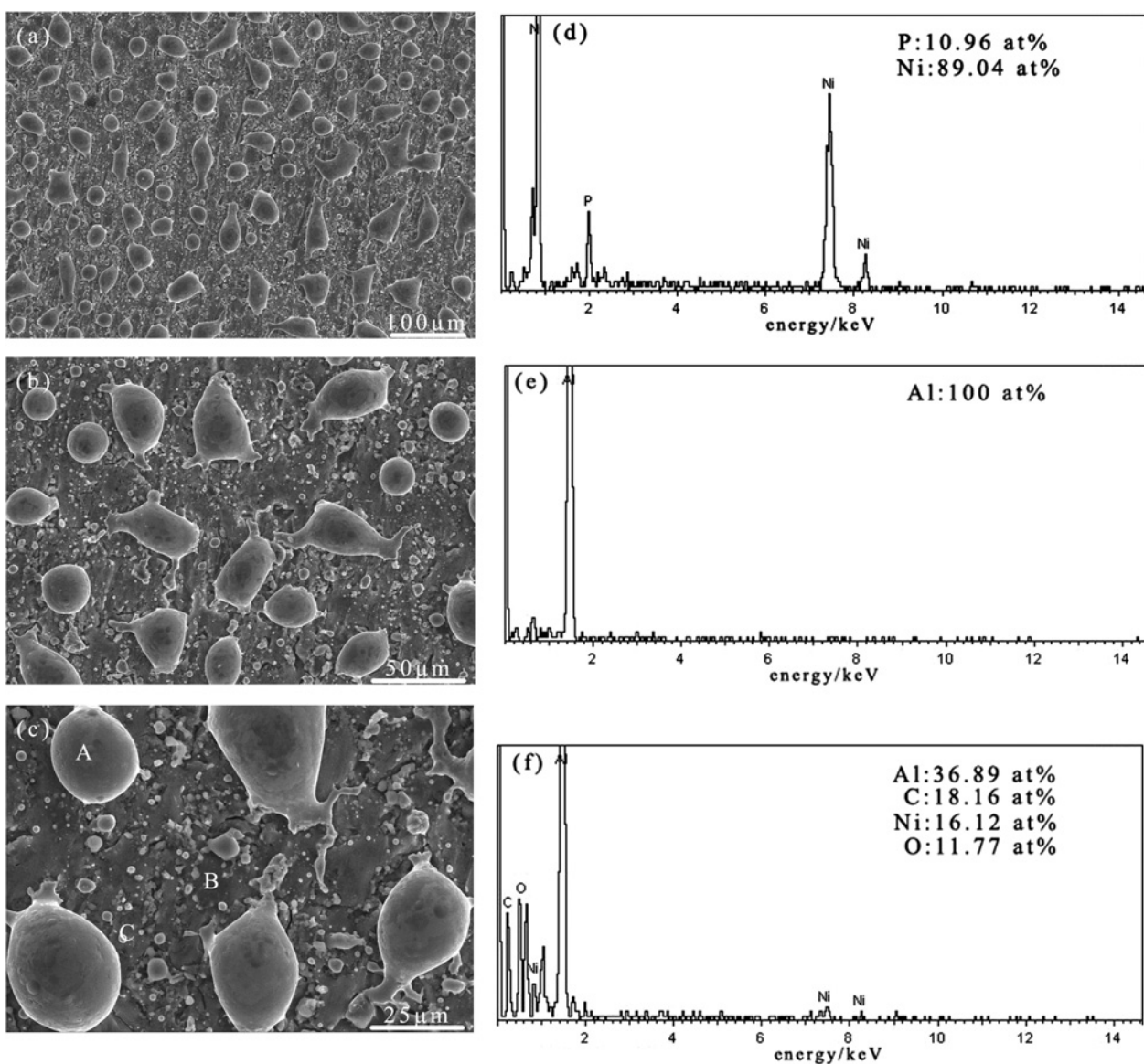


**Fig. 3** Surface SEM images after electron beam irradiation at different magnification  
*a* 100  $\mu\text{m}$   
*b* 50  $\mu\text{m}$   
*c* 25  $\mu\text{m}$   
*d* EDS of point A  
*e* EDS of point B and  
*f* EDS of point C

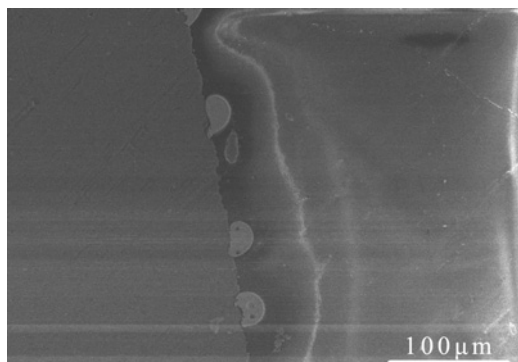


Fig. 4 Cross-section SEM images after electron beam irradiation

homogeneous central part. During the electron beam treatment process the accelerating voltage was 10 kV, pulse current of 100 A, pulse duration of 30  $\mu$ s, beam's diameter of 60 mm and pulse number of 15. The working gas (air) pressure in the chamber was  $2.5 \times 10^{-2}$  Pa.

Surface microstructure of the specimens was characterised by a HITACHI S3400 SEM. An EDS attached to the SEM was also employed to analyse chemical compositions of local positions. In addition, the phase constituents of the specimens were determined by an XRD with a Rigaku D/max-RB (Japan) diffractometer, utilising Cu K $\alpha$  radiation.

**3. Results and discussion:** Fig. 1 shows the surface morphology image of LY12 Al alloy polished with SiC paper. Some micropores and the slurry flow directions can be observed. The surface of the substrate is uniform.

The typical surface morphology of the electroless Ni-P layer is shown in Fig. 2a. The electroless Ni-P alloy layer is uniform and compact and exhibits a typical spherical nodular structure. It is also seen that the individual Ni-P nodule is composed of numerous sub-micro particles. Fig. 2b shows the cross-section morphology of the Ni-P layer plating on the LY12 Al alloy substrate. The total thickness of the Ni-P layer is 2.3  $\mu$ m. The mass fraction of P in the layer prepared in this work analysed by EDS as shown in Fig. 2c is around 8.26%. This implies that the obtained Ni-P layer is likely to be the mixture of amorphous and microcrystalline structure [13], which would be further confirmed by XRD.

The effect of HCPEB on the morphology of the surface layer is evaluated by SEM. Fig. 3 shows a top view of electron beam irradiated on Ni-P layer at different magnifications. As shown in Fig. 3a, the surface of the sample exhibits round, elliptical, fish-like particles which are homogeneously distributed throughout the substrate surface. The size of these particles ranges from 1 to 45  $\mu$ m (see Fig. 3c). Under exposure to HCPEB, Ni-P layer was melted into low viscosity liquid. Due to the poor compatibility of the Ni-P melt with the LY12 Al alloy surface, just like that of the water droplet on the glass with keeping unwetted state, the melt quickly moved to a wide variety of shapes and sizes. The liquid Ni-P gathered and maintained the morphology during rapid cooling process.

As demonstrated in EDS spectrum (Fig. 3d) that the Ni-P is only found in the aggregated regions, while the area without aggregation of Ni-P contains Al (Fig. 3e) or Al, Ni, C and O elements (Fig. 3f).

Fig. 4 shows the cross-sectional SEM images of the sample after HCPEB irradiation. It can be seen clearly that the white-bright remelted layer was formed on the surface of LY12 Al alloy. Also, some spherical particles were impacted into the region between the substrate and the remelted layer.

Fig. 5 shows XRD patterns of specimens with and without HCPEB irradiation. When compared to that of the initial LY12 Al alloy, the surface layer of the specimen after electron beam

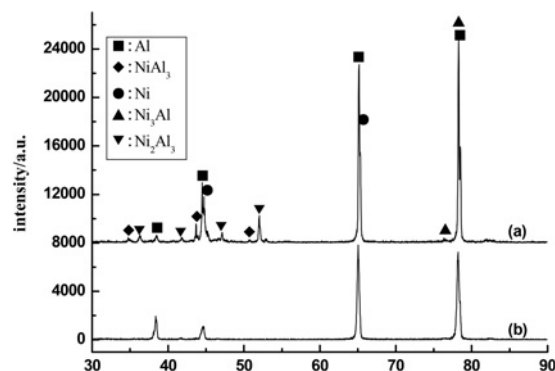


Fig. 5 Diffraction patterns of the surface layers of specimen after a) Electron beam irradiation and b) Initial LY12 Al alloy substrate

irradiation is dominated by Al and resolidification layer of Ni-P.  $Al_3Ni$ ,  $AlNi_3$  and  $Al_3Ni_2$  can also be detected on the surface of the specimen. The possible reason of this phenomenon is that the position of the detector is too close to the substrate of specimens, due to the electron beam irradiation, and the content of Ni-Al is closer to  $Al_3Ni$ ,  $AlNi_3$  or  $Al_3Ni_2$ . Besides that, corresponding EDS results of Fig. 3f (point C) exhibit that the composition of the remelted surface layer was also mixed carbon oxides.

**4. Conclusion:** Ni-P layer was successfully deposited on LY12 substrate by electroless plating method and then this Ni-P layer was irradiated by HCPEB. The produced specimens were investigated using SEM, EDS and XRD in order to observe the microstructure and morphology. Ni-P layer was melted into low viscosity liquid and quickly moved to a wide variety of shapes and sizes under exposure to HCPEB irradiation because of surface unwetting. The surface area was dominated by Al and resolidification layer of Ni-P.  $Al_3Ni$ ,  $AlNi_3$  and  $Al_3Ni_2$  could also be detected on the surface of the specimen.

**5. Acknowledgements:** The authors thank General Program of Natural Science Foundation of China (grant no. 51472048), International Cooperation Project (grant no. F16-214-6-00) and General Project of Science and Technology Research Project (grant no. F15-199-1-18) from Shenyang City Department of Science and Technology for financial support. Partial support from Foundation of Science and Technology (grant no. 20170540780) of Liaoning Provincial Department of Science and Technology was also gratefully acknowledged.

## 6 References

- [1] Adabi M., Amadeh A.A.: 'Formation mechanisms of Ni-Al intermetallics during heat treatment of Ni coating on 6061 Al substrate', *Trans. Nonfer. Met. Soc.*, 2015, **25**, (12), pp. 3959–3966
- [2] Krasnowski M., Gierlotka S., Kulik T.: 'Nanocrystalline matrix  $Al_3Ni_2$ -Al- $Al_3Ni$  composites produced by reactive hot-pressing of milled powders', *Intermetallics*, 2014, **54**, pp. 93–98
- [3] Krasnowski M., Gierlotka S., Kulik T.: ' $Al_3Ni_2$ -Al composites with nanocrystalline intermetallic matrix produced by consolidation of milled powders', *Adv. Powder. Technol.*, 2014, **25**, (4), pp. 1362–1368
- [4] Parsa M.R., Soltanieh M.: 'On the formation of  $Al_3Ni_2$  intermetallic compound by aluminothermic reduction of nickel oxide', *Mater. Charac.*, 2011, **62**, (7), pp. 691–696
- [5] Hao S., Li M.: 'Producing nano-grained and Al-enriched surface microstructure on AZ91 magnesium alloy by high current pulsed electron beam treatment', *Incl. Instr. Methods B*, 2016, **375**, pp. 1–4
- [6] Meisner L.L., Markov A.B., Proskurovsky D.I., *ET AL.*: 'Effect of inclusions on cratering behavior in TiNi shape memory alloys

- irradiated with a low-energy, high-current electron beam', *Surf. Coat. Technol.*, 2016, **302**, pp. 495–506
- [7] Meisner L.L., Lotkov A.I., Ostapenko M.G., *ET AL.*: 'X-ray diffraction study of residual elastic stress and microstructure of near-surface layers in nickel-titanium alloy irradiated with low-energy high-current electron beams', *Surf. Coat. Technol.*, 2013, **280**, pp. 398–404
- [8] Neiman A.A., Meisner L.L., Lotkov A.I., *ET AL.*: 'Cross-sectional TEM analysis of structural phase states in TiNi alloy treated by a low-energy high-current pulsed electron beam', *Appl. Surf. Sci.*, 2015, **327**, pp. 321–326
- [9] Luo D., Tang G., Ma X., *ET AL.*: 'The microstructure of Ta alloying layer on M50 steel after surface alloying treatment induced by high current pulsed electron beam', *Vacuum*, 2017, **136**, pp. 121–128
- [10] Chai L., Chen B., Wang S., *ET AL.*: 'Microstructural, textural and hardness evolution of commercially pure Zr surface-treated by high current pulsed electron beam', *Appl. Surf. Sci.*, 2016, **390**, pp. 430–434
- [11] Chai L., Zhou Z., Xiao Z., *ET AL.*: 'Evolution of surface microstructure of Cu-50Cr alloy treated by high current pulsed electron beam', *Sci. Chin. Technol. Sci.*, 2015, **58**, (3), pp. 462–469
- [12] Zhou Z., Chai L., Xiao L., *ET AL.*: 'Surface modification of Cu-25Cr alloy induced by high current pulsed electron beam', *Trans. Nonferr. Met. Soc. Chin.*, 2015, **25**, (6), pp. 1935–1943
- [13] Sun C., Guo X., Wang S., *ET AL.*: 'Homogenization pretreatment and electroless Ni-P plating on AZ91D magnesium alloy', *Trans. Nonferr. Met. Soc.*, 2014, **24**, (12), pp. 3825–3833